COMPARATIVE STUDY BETWEEN PLASMA AND LASER CUTTING OF STEELS AND POLYMERIC MATERIALS

Daniel Ghiculescu[1], Liviu Nita[2], Jozsef Pop[3] and Andrei Rusu[4]
[1] Polytechnic University of Bucharest, Faculty of Industrial Engineering and Robotics, daniel.ghiculescu@upb.ro
[2] Polytechnic University of Bucharest, Faculty of Industrial Engineering and Robotics, nita.liviu98@gmail.com
[3] Polytechnic University of Bucharest, Faculty of Industrial Engineering and Robotics, pop.jozsef99@gmail.com[3]
[4] Polytechnic University of Bucharest, Faculty of Industrial Engineering and Robotics, andreirusu245@yahoo.com

ABSTRACT: The paper deals with comparative study between plasma and laser cutting of different materials. C 45 and stainless steel were cut by these mentioned above technologies with different working parameters. The surface quality was studied using scanning electron microscopy. The comparison was extended in the same manner, at laser cutting of some polymeric materials like PVC and Plexiglas. COMSOL Multiphysics, Heat transfer module was used in a dynamic variant with a sweep parameter as machining time in connection to feed rate, aiming at improvement of output technological parameters at plasma and laser cutting. A Gaussian distribution of the energy on laser and plasma spot was introduced as boundary conditions, as well as thermal characteristics of the studied materials. The quality of machined surface was considered based on moderate heating of the material. Some values of working parameters were established due to computerized modelling. These were validated by experimental results.
KEYWORDS: plasma, laser cutting, steels, polymers, FEA.

1. INTRODUCTION

Plasma cutting / plasma machining – PM) has become nowadays one the of the most used nonconventional technologies due to its relatively low costs and capacity to machine electrically conductive materials as anode, no matter their hardness. PM is challenging laser cutting / laser beam machining - LBM in terms of costs and thickness of machined workpiece [1] but is inferior to LBM, due to the range of material to be cut, with practically almost no limits. LBM still has dominance too owing to its superior energy and capacity of focusing it on machined surface. Thus, it creates the highest power density in industrial applications, $J=10^{14}$ W/cm^2. For comparison, the most used nonconventional technology, electrical discharge machining – EDM achieves in plasma channel, $J=10^{10}$ W/cm^2 [2].

All these studied technologies have the advantage of high machining rate and flexibility by CNC using, but the disadvantage of low surface quality comparing to other conventional, e. g. diamond burnishing [3] or EDM and ECM, but the last ones are only restricted to electrically conductive materials [2].

Nevertheless, research on plasma cutting highlights widening and improvements of specific equipment, including portable ones [4]. Similar studies were approached on plasma cutting of different steels [5]. Significant research was also conducted to improve some drawbacks of plasma cutting, namely the precision at various steels cutting [6].

Recent studies were oriented to laser cutting of plastic materials to ameliorate some of the disadvantages, e. g. fume emissions at polyvinyl chloride [7], improving precision and surface roughness at acrylonitrile butadiene styrene [8], and 3D-printed PET-G plates cutting [9].

2. MODELING OF THERMAL PROCESSES OF PLASMA AND LASER CUTTING ON DIFFERENT MATERIALS

Since all the technologies that were approached are thermal ones, we attempted to create a versatile model that could be applied on specific cases that are the subject of this comparative study.

COMSOL Multiphysics, Heat transfer module, Time dependent mode were used for finite element modelling of the plasma and laser cutting processes.

The following stages were covered, presented in detail below:

(1) parameterization of the models;

(2) the geometry of the models;

(3) materials properties;

(4) boundary conditions (physics characterization);

(5) mesh of the models;

(6) sweep and time dependent parameters;

(7) running of the models;

(8) visualization of the results;

(9) simulation of the cutting processes.

(1) Three different processes were studied comparatively in terms of heat source and material type: plasma cutting of steels, laser cutting of steels, laser cutting of plastic materials. Their parameters addressing heat source, its kinematics, machined sample geometry, and thermal characteristics of material behavior are exemplified in figure 1:

Name	Expression	Value	Description
P	14000[W]	14000 W	plasma power
dspot	0.2[mm]	2E-4 m	plasma spot diameter [μm]
sigma	dspot/6	3.3333E-5 m	mean square deviation
Ed	P/(pi*0.25*dspot^2)	4.4563E11 W/m²	power density on plasma spot
speed	5[m/min]	0.083333 m/s	cutting speed [m/s]
rmgaz	0.1[mm]	1E-4 m	radius of gas margin
xr	x0+speed*tp	2E-4 m	mobile reference spot
x0	rmgaz+dspot/2	2E-4 m	reference distance from laser spot center
tstop	(l1-2*0.2*rgaz)/speed	0.1104 s	machininig time [s]
tp	0[s]	0 s	sweep machining time
l1	10[mm]	0.01 m	sample width
l2	20[mm]	0.02 m	sample length
gp	2[mm]	0.002 m	sample height
emi	0.25	0.25	steel emissivity coefficient
A1	0.56	0.56	steel absorption coefficient
h1	10[W/(m^2*K)]	10 W/(m²·K)	heat transfer coefficient
Ttop304	1400+273.15	1673.2	melting point of stainless steel 304

a) Parameters for plasma cutting of stainless steel

Parameters

Name	Expression	Value	Description
P	1000[W]	1000 W	laser power
dspot	0.015[mm]	1.5E-5 m	laser spot diameter [μm]
sigma	dspot/6	2.5E-6 m	mean square deviation
Ed	P/(pi*0.25*dspot^2)	5.6588E12 W/m²	power density on laser spot
speed	3[m/min]	0.05 m/s	laser speed [m/s]
xr	x0+speed*tp	0.002 m	mobile reference spot
x0	rgaz	0.002 m	reference distance from laser spot center
tstop	(l1-2*rgaz)/speed	0.12 s	cutting time [s]
tp	0[s]	0 s	sweep machining time
rgaz	2[mm]	0.002 m	gas spot radius
l1	10[mm]	0.01 m	sample width
l2	20[mm]	0.02 m	sample length
gp	2[mm]	0.002 m	sample height
A1	0.1	0.1	steel absorption coefficient
emi	0.9	0.9	steel emissivity coefficient
h1	10[W/(m^2*K)]	10 W/(m²·K)	heat transfer coefficient
Ttop304	1700	1700	melting point of stainless steel 304

b) Parameters for laser cutting of stainless steel

Name	Expression	Value	Description
P	24.6[W]	24.6 W	laser power
dspot	0.12566[mm]	1.2566E-4 m	laser spot diameter
sigma	dspot/6	2.0943E-5 m	mean square deviation
Ed	P/(pi*0.25*dspot^2)	1.9836E9 W/m²	power density on laser spot
speed	8.877[mm/s]	0.008877 m/s	feed speed [m/s]
tstop	(l1-2*rgaz)/speed	1.0139 s	machining time [s]
tp	0[s]	0 s	sweep machining time
rgaz	0.5[mm]	5E-4 m	gas spot radius
x0	rgaz	5E-4 m	reference distance from laser spot center
xr	x0+speed*tp	5E-4 m	mobile reference spot
l1	10[mm]	0.01 m	sample width
l2	20[mm]	0.02 m	sample length
gp	2[mm]	0.002 m	sample heigth
emi	0.89	0.89	emissivity coefficient
A1	0.28	0.28	absorption coefficient
h1	10[W/(m^2*K)]	10 W/(m²·K)	heat transfer coefficient
TtopPVC	177+273.15	450.15	melting point of PVC [K]

c) Parameters for laser cutting of PVC

Figure 1. Examples of parameters used of the cutting models

(2) The geometry 2D was created using Comsol built-in tools, considering the machined sample overall dimensions, the dimensions and movement of the plasma / laser spot and assisting gas spot (figure 2).

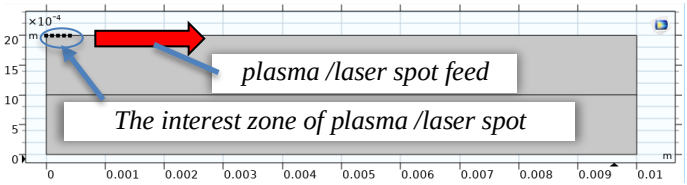

(a) The geometry 2D of machined sample – general view

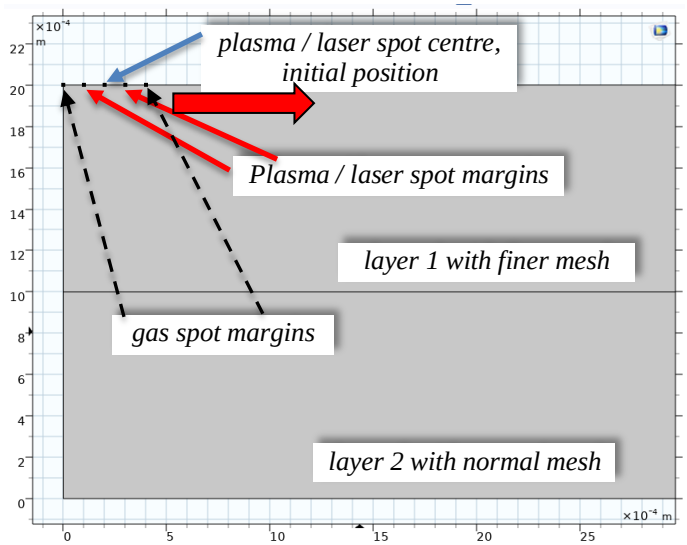

(b) the laser/plasma spot and gas margins – interest zone

Figure 2. The generic geometry of the models

Two layers are created for different meshing. The models are dynamic, based on sweep parameter as machining time that depends on the cutting speed. Thus, the laser spot covers the superior face of the sample from left to right aiming at cutting the material on the entire depth, at high surface quality without overheating or underheating (incomplete cutting).

(3) Material properties related to thermal calculation are allocated from Comsol library, as it is exemplified in figure 3, in case of stainless steel 304, PVC and Plexiglas (Poly(methyl methacrylate - (PMMA).

	Property	Variable	Value	Unit
✓	Thermal conductivity	k_iso ; kii = k_iso, kij = 0	16.2	W/(m·K)
✓	Density	rho	8000	kg/m³
✓	Heat capacity at constant pressure	Cp	502	J/(kg·K)

(a) stainless steel properties

	Property	Variable	Value	Unit
✓	Density	rho	1760[kg/m^3]	kg/m³
✓	Thermal conductivity	k_iso ; kii = k_iso, kij = 0	0.1[W/(m*K)]	W/(m·K)
✓	Heat capacity at constant pressure	Cp	880	J/(kg·K)

(b) PVC properties

	Property	Variable	Value	Unit
✓	Density	rho	1180[kg/m^3]	kg/m³
✓	Thermal conductivity	k_iso ; kii = k_iso, kij = 0	0.18[W/(m*K)]	W/(m·K)
✓	Heat capacity at constant pressure	Cp	1700	J/(kg·K)

(c) Plexiglas properties

Figure 3. Materials properties allocation

(4) The boundary conditions were set using some variable definitions which suppose a Gaussian distribution on laser spot [10], and similar on plasma spot [11], as it is presented in figure 4.

Name	Expression	Unit	Description
G_space	exp(-(x-xr)^2/(2*sigma^2))		Gauss distribution of energy on laser spot
Plaser	A1*Ed	W/m²	power density absorbed
LHS	Plaser*G_space	W/m²	power density distribution on laser spot

Figure 4. Variables definitions related to Gaussian distribution

The plasma and laser spots were set, using the variable definitions from above – figure 5.

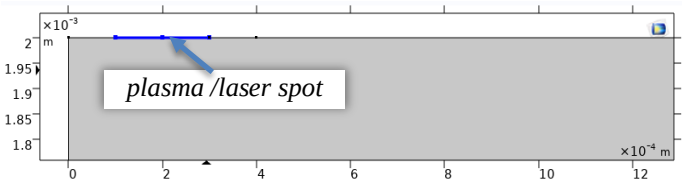

Figure 5. Heat source allocation on plasma / laser spot

Thermal insulation was considered on the spot occupied by assisting gas as indicated in figure 6.

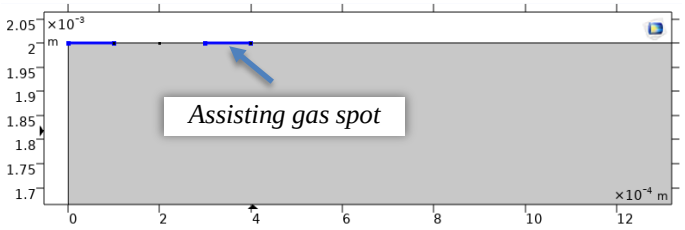

Figure 6. Thermal insulation on assisting gas spot

The cooling and radiation at ambient temperature were allocated to surfaces shown in figure 7, and 8.

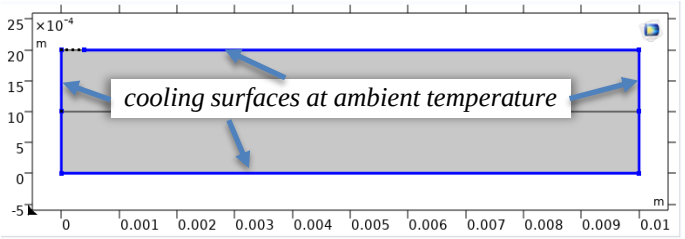

Figure 7. Cooling at ambient temperature, 293,15K with heat transfer coefficient, *h1*

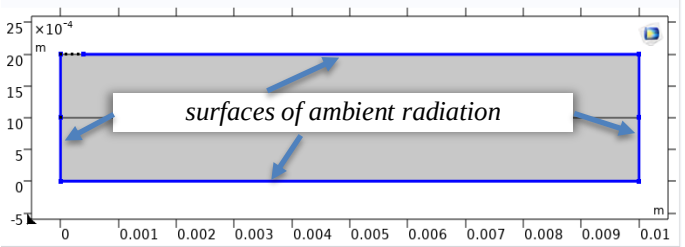

Figure 8. Surfaces to ambient radiation, 293,15K through surface emissivity coefficient, *emi*

(5) The mesh was dynamic during the displacement of the heat source, and differentiated using two layers, with different sizes of the free triangular elements, extra fine on the interest zone, and normal in rest, as it is presented in figure 8, along with the quality scale.

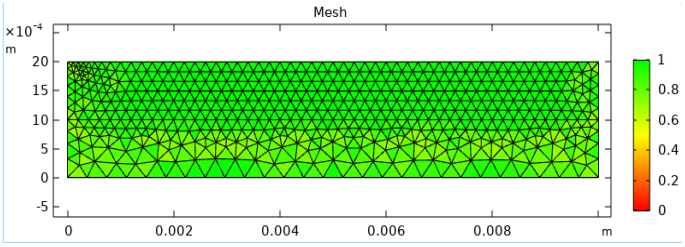

Figure 9. Mesh disposal and its corresponding quality scale

(6) The sweep parameter and the time dependent one were assigned as *tp* (see models parameters – figure 1) and respectively, *tstop*, for building the dynamic models of the cutting process by plasma and laser.

(7) The parameters *tp* and *tstop* are the required parameters for the stage of solving the models.

(8) The results obtained highlighted the thermal front that covers partially at a certain moment, the transversal section of the sample – figures 10 - 15. Thus, the cutting of the entire section is achieved by appropriate values of the working parameters, avoiding overheating or underheating, and surface quality assured.

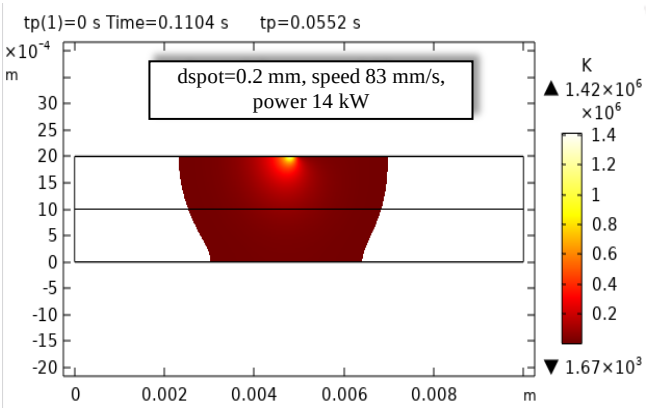

Figure 10. The thermal front dynamics during machining at plasma cutting of stainless steel 305

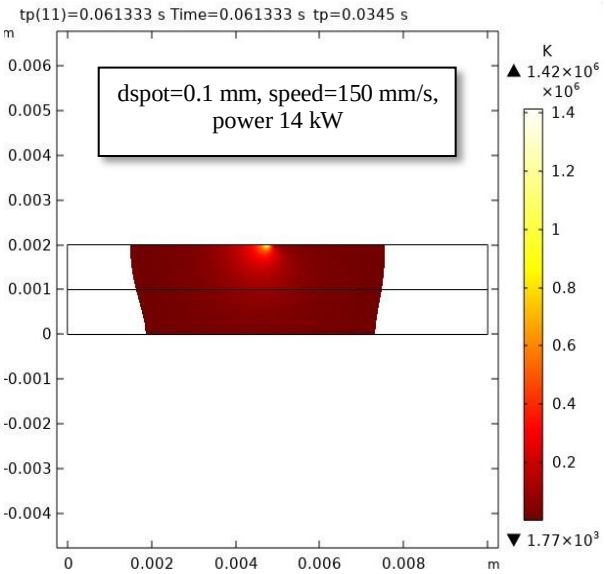

Figure 11. The thermal front dynamics during machining at plasma cutting of steel C45

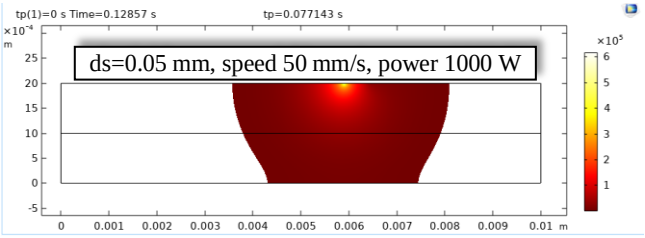

Figure 12. The thermal front dynamics during machining at laser cutting of stainless steel 305

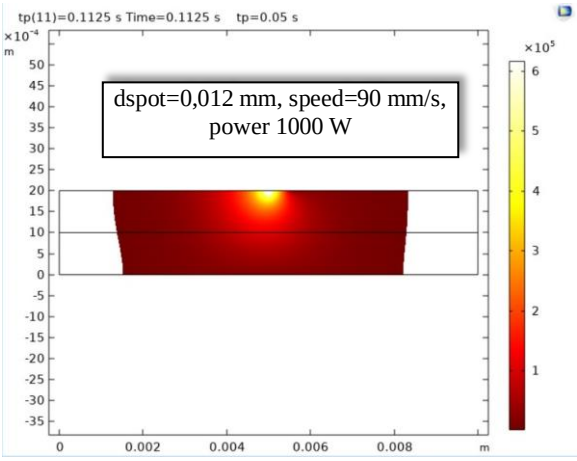

Figure 13. The thermal front dynamics during machining at laser cutting of steel C45

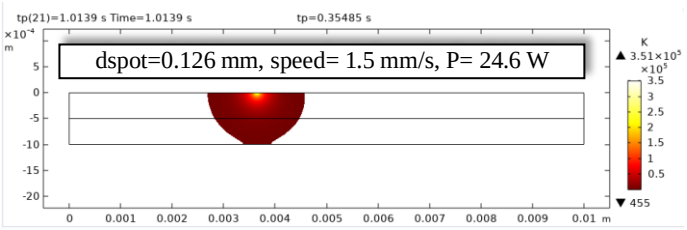

Figure 14. Thermal front dynamics at laser cutting of PVC

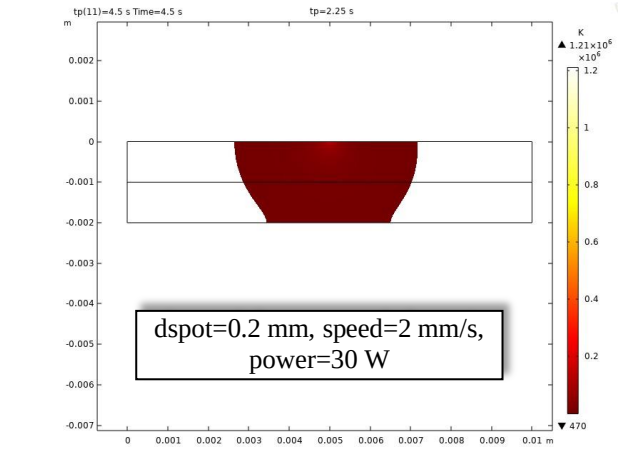

Figure 15. Thermal front dynamics at laser cutting of Plexiglas

(9). The simulations from figures 10-15 pointed out that the type of cutting and machined materials required the adjustments of working parameters: higher power at plasma cutting than laser cutting due to focusing capacity at LBM; the diameter of the heat source at LBM is of 0.01 mm order of magnitude in comparison with PM, which is of 0.1 mm; the power is much lower at plastic materials, comparing to steels cutting with a slight increase and lower cutting speed at Plexiglas than PVC; the cutting speed is decreased at stainless steel in comparison with C 45, both at plasma and laser cutting.

3. PLASMA AND LASER CUTTING EXPERIMENTS

The tests for plasma cutting of stainless steel and C45 steel were effectuated on Powermax105 SYNC, whose technical data are presented in table 1.

Table 1. Technical data of the Powermax105 SYNC Plasma cutting machine

Generator power [kW]	Maximum 30 kW for 105A current
Voltage [V]	380
Current intensity [A]	35 - 105
Gas supply	Clean, dry air, no oil or oxygen
Optimum intake gas pressure [MPa]	0.76–0.83
Minimum inlet gas pressure [MPa]	0.46
Type of power supply	IGBT Inverter (Bipolar Transistor with isolated deck)

The laser cutting of the same mentioned above steels was done on laser Bodor i7 1kW, its characteristics being presented in table 2.

Table 2. Technical data of Bodor i7 1kW laser

Laser source power [W]	1000
Mode of operation	Continuous/modulated
Wavelength [nm]	1080±10
Laser beam quality	≤1.5mm x mrad (50µm QBH)
Frequency [kHz]	≤20
Diameter of optical fiber [µm]	50, doped with ytterbium
Laser spot diameter [mm]	Focalization depending on thickness
Maximum thickness [mm]	12 (steel)

The samples from PVC and Plexiglass were cut on laser installation, NOVA 51.

Table 3. Technical data of NOVA51laser

Laser source power [W]	100-130
Mode of operation	Continuous/modulated
Wavelength [nm]	1080±10
Frequency [kHz]	≤5
Laser spot diameter [mm]	Focalization depending on thickness
Maximum thickness [mm]	10 (polymeric materials)

The machined surfaces were studied by scanning electron microscope (SEM) QUANTA INSPECT F50 SEM, resolution of 1 nm and presented in figures 16-21. An obvious superior quality was observed at laser compared to plasma cutting of studied steels. Moreover, the quality at stainless steel 304 is apparent superior to C45. Entrance and exit zones with depths of 0.1 mm magnitude order were identified, where the quality was inferior to that obtained in center zones.

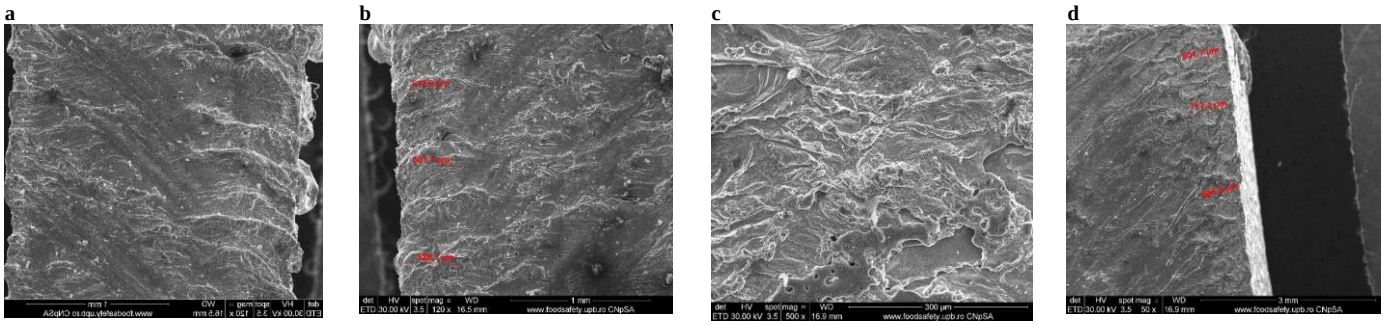

Figure 16. Plasma cutting of stainless steel 304, 2 mm thickness,
v = 83 mm/s, gas pressure, p = 0.5 MPa, current I=35A, power P = 14 kW; a) general view, b) entrance, c) middle, d) exit

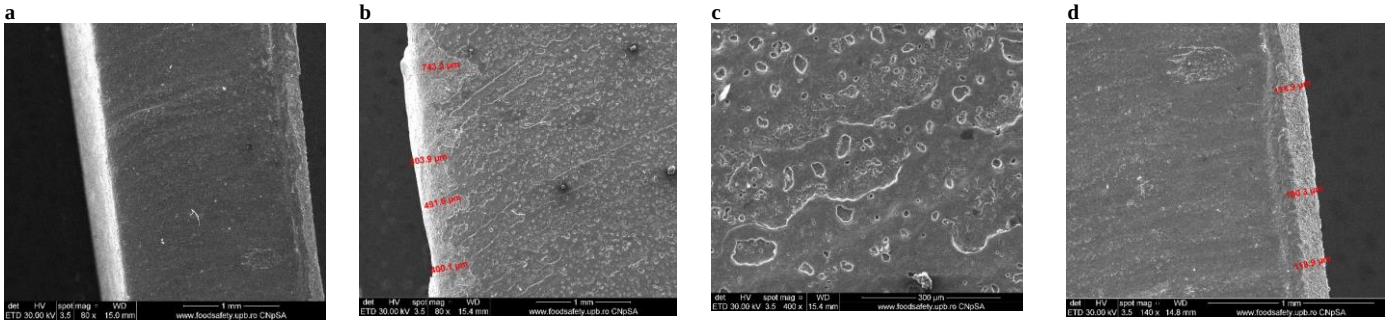

Figure 17. Plasma cutting of steel C45, 2 mm thickness,
v = 150 mm/s, gas pressure, p = 0.5 MPa, current I=35A, power P = 14 kW; a) general view, b) entrance, c) middle, d) exit

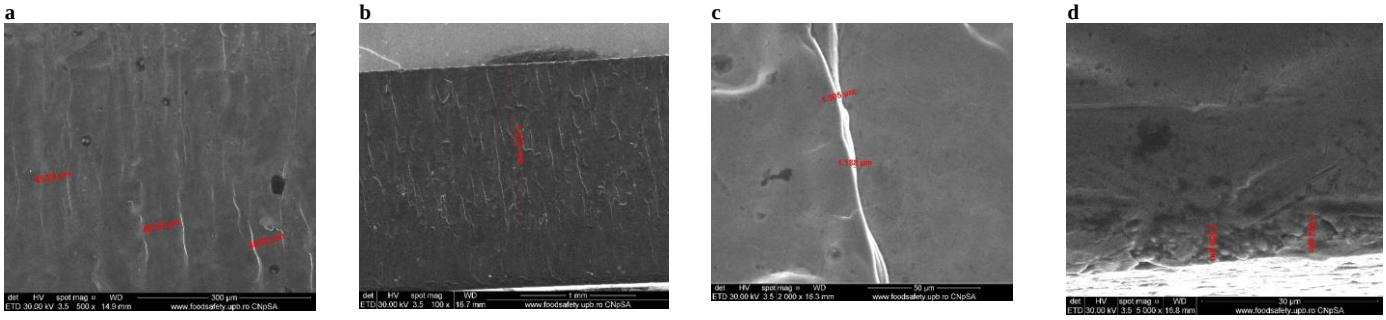

Figure 18. Laser cutting of stainless steel 304, 2 mm thickness,
cutting speed, v=50 mm/s, power P=1000 W; a) general view, b) entrance, c) middle, d) exit

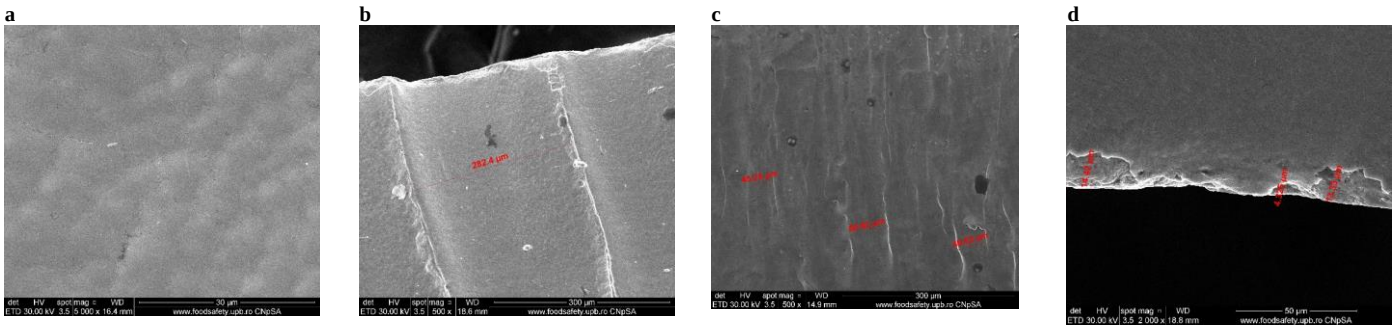

Figure 19. Laser cutting of steel C45, 2 mm thickness,
cutting speed, v=90 mm/s, power, P=1000 W; a) general view, b) entrance, c) middle, d) exit

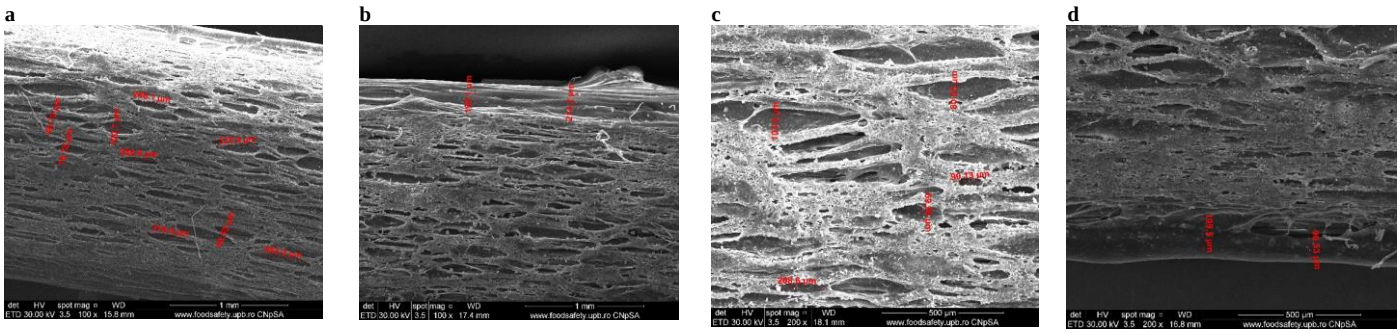

Figure 20. Laser cutting of PVC, 2 mm thickness,
cutting speed, v=1.5 mm/s, power, P=24.6 W; a) general view, b) entrance, c) middle, d) exit

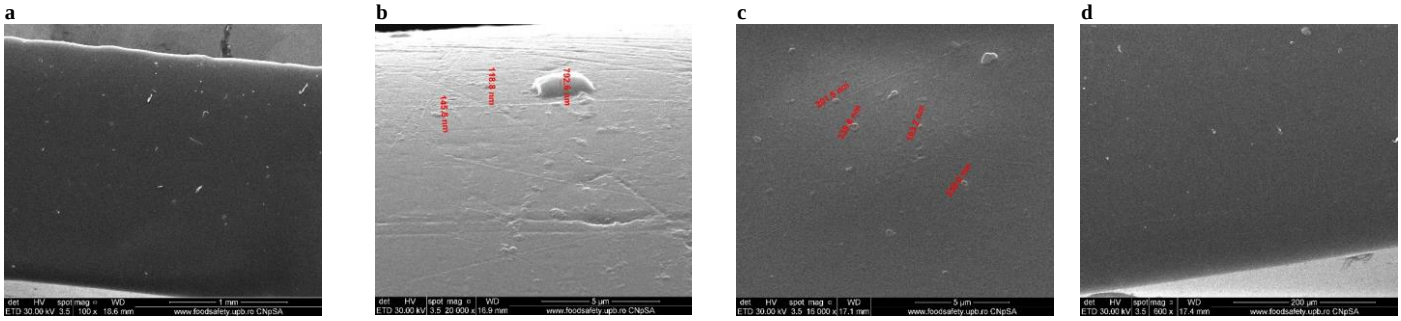

Figure 21. Laser cutting of Plexiglass, 2 mm thickness,
cutting speed, v=2 mm/s, power, P=30 W; a) general view, b) entrance, c) middle, d) exit

At laser cutting of PVC, the surface quality is inferior to Plexiglas because of many microcavities with dimensions of 0.2-0.3 mm formed on cut surfaces. There are also entrance and exit zones with inferior quality of around 0.2 mm compared to the center of the cut surfaces. At Plexiglas only some holes and bumps with than less 1 µm diameters are highlighted.

4. CONCLUSIONS

Numerical simulations of cutting aiming at moderate heating, validated experimentally, emphasized the influence of the heat source. The power needed at plasma cutting is much greater than at laser, due to laser spot diameter, of 1 order of magnitude smaller than the plasma one. The influence of cut materials at laser use is also highlighted: the steels machining requires obviously more power than plastic materials.

SEM images analysis pointed out that surface quality at laser cutting is obviously superior to plasma use. Laser cutting of stainless-steel shows higher surface quality than in case of usual C45 steel, with less structural damages produced by temperature gradient. Similar phenomena were revealed at laser cutting of plastics, Plexiglass behavior being superior to PVC. Surface quality is not uniform on the entire depth of cutting. There are entrance and exit zones of 0.1 mm magnitude order for all studied materials, where the quality is inferior to the center zones.

Further research will approach 3D numerical simulations and experiments of the cutting processes, considering the dynamic influence of the gap geometry created by material evacuation.

5. ACKNOWLEDGEMENTS

The SEM images were possible due to EU-funding project POSCCE-A2-O2.2.1-2013-1.

6. REFERENCES

1. Krajcarz, D., Comparison Metal Water Jet Cutting with Laser and Plasma Cutting, *Procedia Engineering*, Vol. 69, pp. 838-843, (2014).
2. Marinescu, N.I. et al., *Technological processes with beams, oscillations, and jets*, Printech, Bucharest, (2019).
3. Varga, G., Ferencsik, V., Analysis of shape correctness of surfaces of diamond burnished components, *Modern Technologies in Manufacturing, MTeM – AMaTUC*, Trans Tech Publications, 137(4):01019, Cluj-Napoca, Romania (2017).
4. Mangaraj, S.R. et al., Experimental study of a portable plasma arc cutting system using hybrid RSM-nature inspired optimization technique, *Materials Today: Proceedings*, Vol. 50, Part 5, Pages 867-878, (2022).
5. Auz C, F.G., et al. Comparative Analysis of Plasma Cutting Parameters Between K100 and W300 Steels, *Innovation and Research - A Driving Force for Socio-Econo-Technological Development*. CI3 2021, Vol. 511. Springer, (2022).
6. Anakhov, S.V., Guzanov, B.N. & Matushkin, A.V., Development of Equipment and Technology for Precision Air-Plasma Cutting of Plate Steel, *Steel Transl.* Vol. 52, pp.19–26 (2022).
7. Elsheikh, A.H., Muthuramalingam, T., Abd Elaziz, M. et al. Minimization of fume emissions in laser cutting of polyvinyl chloride sheets using genetic algorithm. *Int. J. Environ. Sci. Technol.*, Vol. 19, pp. 6331–6344 (2022)
8. Kechagias, J.D., Ninikas, K., Petousis, M. et al. Laser cutting of 3D printed acrylonitrile butadiene styrene plates for dimensional and surface roughness optimization. *Int. J. Adv. Manuf. Technol*. Vol. 119, pp. 2301–2315 (2022).
9. Kechagias, J.D. et al. Surface characteristics investigation of 3D-printed PET-G plates during CO_2 laser cutting, *Materials and Manufacturing Processes*, Vol. 37, Issue 11, (2022).
10. Vora, H.D., et al. One-dimensional multipulse laser machining of structural alumina: evolution of surface topography. *Int. J. Adv. Manuf. Technol*. Vol. 68, 69–83 (2013).
11. Hirvijoki, E. et al., The Gaussian radial basis function method for plasma kinetic theory, *Physics Letters A*, Vol. 379, Issue 42, pp. 2735-2739, (2015).